Consideration of the yarn–yarn interactions in meso/macro discrete model of fabric Part II: Woven fabric under uniaxial and biaxial extension

Bilel Ben Boubaker [b,*], Bernard Haussy [b], Jean-François Ganghoffer [a,1]

[a] *LEMTA, UMR 7563, ENSEM, 2, Avenue de la Forêt de Haye, BP 160, 54504 Vandoeuvre Cedex, France*
[b] *ESEO, 4, rue Merlet de la Boulaye, 49009 Angers Cedex 01, BP 926, France*

Available online 14 February 2007

Abstract

A mesoscopic discrete model of fabric has been developed, accounting for the yarn–yarn interactions occurring at the yarn crossing points. The fabric yarns, described in their initial state by a Fourier series development, are discretized into elastic straight bars represented by stretching springs, and connected at frictionless hinges by rotational springs. In the first part of the paper, the behavior under uniaxial tension of a single yarn has been investigated, and the impact of the interactions of the transverse yarns has been quantitatively assessed. The consideration of the yarn interactions is extended in this second part at the scale of the whole network of interwoven yarns, under uniaxial and biaxial loading conditions. The effect of the transverse yarns properties under uniaxial tension is evidenced, as well as the impact of the biaxial loading ratio.
© 2007 Elsevier Ltd. All rights reserved.

Keywords: Woven structures; Discrete models; Traction curve; Yarn–yarn interactions; Uniaxial and biaxial extensions

1. Analysis of woven fabric behavior under uniaxial extension

We have developed a discrete mass-spring model of the mesoscopic mechanical behavior of a woven structure, taking into account the yarn–yarn interactions at the mesoscopic scale. From the literature review given in Part I, we can observe that few works deal with discrete modeling of woven structures: the works by Provot (1995) and Magno and Lutz (2002), fall within this kind of approach.

The stiffening effect of the yarn–yarn interactions on the fabric mechanical behavior has been evidenced, and the traction curve of a single yarn has been simulated, reproducing thereby the observed J-shaped curve.

---

* Corresponding author. Tel.: +33 0241866735; fax: +33 0241879927.
E-mail addresses: bilel.ben_boubaker@eseo.fr (B.B. Boubaker), bernard.haussy@eseo.fr (B. Haussy), jfgangho@ensem.inpl-nancy.fr (J.-F. Ganghoffer).
[1] Tel.: +33 0383595724; fax: +33 0383595551.

The deformation mechanisms of the yarn consists of flexional contribution, being attributed to a change of its undulation and an extension; the flexional displacement is shown to tend towards a saturation value, whereas the extensional displacement monotonously increases vs. the applied traction load. This discrete methodology is further extended in this second part to analyze the structural behavior at the scale of the woven structures under uniaxial and biaxial loadings.

The set of intertwined yarns Ω is decomposed into the assembly of two sub-mechanical systems (Fig. 1), namely the set of warp yarns, Ω_{wa}, being in interaction with the set of weft Ω_{we}, here considered as an external (sub-mechanical) system.

In order to study the effect of the parameters of the structure (applied loads, yarns' mechanical properties) on the extension behavior of the woven structure, the mechanical behavior of the mechanical system Ω is first analyzed in the warp direction (x-direction). For that purpose, the total potential energy associated to the warp yarns' system Ω_{wa} is first established. Under the extension loads, the deformed shape of a warp yarn of index k is assumed to retain its initial periodical shape, expressed as the following Fourier series:

$$w_{\text{wa}}^k(x) = \sum_{n=1}^{N_{\text{we}}} a_{n,k}^{\text{wa}} \sin\left((k-1)\pi + n\frac{\pi x}{L_{\text{wa}}}\right) \tag{1}$$

Under the effect of the loads P_{wa} and P_{we} applied, respectively in the warp and weft directions (supposed to be uniformly distributed along the edge nodes), an undulation transfer due to the yarn–yarn interaction occurs at the contact points; this undulation transfer process is followed by a lateral displacement of the contact points (Fig. 6, Part I). The displacement continuity occurring at the crossing points labeled by the set of indices (j,k) then expresses as (see relation (23) of Part I for the case of a single yarn)

$$w_{s-\text{we}}^{j,k} = w_{so-\text{we}}^{j,k} + w_{s-\text{wa}}^{j,k} - w_{so-\text{wa}}^{j,k} \tag{2}$$

where j is the index of the weft yarn and k the index of the warp yarn. From the relation (20) of Part I (obtained from the application of beam theory of Timoshenko (1947)), which gives the expression of the reaction force exerted by the warp yarns on the weft yarn in the case of a biaxial extension and using the previous relation (1), we get

$$R_{\text{wa/we}}^{j,k} = \frac{\pi^4}{2} \frac{(EI)_{\text{we}}}{\left(L_p^{\text{we}}\right)^3}\left(1 + \frac{\alpha_{\text{we}}}{N_{\text{wa}}^2}\right)\left[\left(w_{so-\text{we}}^{j,k} - w_{so-\text{wa}}^{j,k}\right) + w_{s-\text{wa}}^{j,k}\right] \tag{3}$$

The action–reaction principle further gives

$$R_{\text{we/wa}}^{j,k} = -R_{\text{wa/we}}^{j,k} = -\frac{\pi^4}{2} \frac{(EI)_{\text{we}}}{\left(L_p^{\text{we}}\right)^3}\left(1 + \frac{\alpha_{\text{we}}}{N_{\text{we}}^2}\right)\left[\left(w_{so-\text{we}}^{j,k} - w_{so-\text{wa}}^{j,k}\right) + w_{s-\text{wa}}^{j,k}\right] \tag{4}$$

The work of the reaction force exerted by a weft yarn of index j on the warp yarn of index k, occurring at the interlacing point (j,k), expresses as
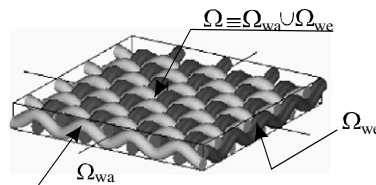

Fig. 1. Woven structure made of two sets of intertwined yarns.

$$W_{R_{\text{we/wa}}^{j,k}} = \int_{w_{so-\text{wa}}^{j,k}}^{w_{s-\text{wa}}^{j,k}} R_{\text{we/wa}}^{j,k}\, dw = \int_{w_{so-\text{wa}}^{j,k}}^{w_{s-\text{wa}}^{j,k}} \left\{ -\frac{\pi^4}{2} \frac{(EI)_{\text{we}}}{\left(L_p^{\text{we}}\right)^3} \left(1 + \frac{\alpha_{\text{we}}}{N_{\text{wa}}^2}\right) \left[\left(w_{so-\text{we}}^{j,k} - w_{so-\text{wa}}^{j,k}\right) + w\right] \right\} dw$$

$$= -\frac{\pi^4}{2} \frac{(EI)_{\text{we}}}{\left(L_p^{\text{we}}\right)^3} \left(1 + \frac{\alpha_{\text{we}}}{N_{\text{wa}}^2}\right)$$

$$\times \left[\left(\left(w_{so-\text{we}}^{j,k} - w_{so-\text{wa}}^{j,k}\right)w_{s-\text{wa}}^{j,k} + \frac{1}{2}w_{s-\text{wa}}^{j,k}{}^2\right) - \left(\left(w_{so-\text{we}}^{j,k} - w_{so-\text{wa}}^{j,k}\right)w_{so-\text{wa}}^{j,k} + \frac{1}{2}w_{so-\text{wa}}^{j,k}{}^2\right)\right] \tag{5}$$

This expression shows the influence of the transversal yarns characteristics EI_{we}, L_p^{we}, $w_{so-\text{we}}$, $w_{s-\text{we}}$ and of the coefficient $\alpha_{\text{we}} = \frac{P_{\text{we}}}{P_{cr}^{\text{we}}}$ – which quantifies the interaction between the two sub-mechanical systems Ω_{wa} and Ω_{we} during the loading – on the work of the reaction force exerted on the warp yarn. Accordingly, the total work of the reaction forces exerted on a warp yarn of index k is given by the sum

$$W_{\text{reaction forces}}^k = \sum_{j=1}^{N_{\text{we}}} W_{R_{\text{we/wa}}^{j,k}} \tag{6}$$

Thus, we get

$$W_{\text{reaction forces}}^k = -\sum_{j=1}^{N_{\text{we}}} \frac{\pi^4}{2} \frac{(EI)_{\text{we}}}{\left(L_p^{\text{we}}\right)^3} \left(1 + \frac{\alpha_{\text{we}}}{N_{\text{wa}}^2}\right)$$

$$\times \left[\left(\left(w_{so-\text{we}}^{j,k} - w_{so-\text{wa}}^{j,k}\right)w_{s-\text{wa}}^{j,k} + \frac{1}{2}w_{s-\text{wa}}^{j,k}{}^2\right) - \left(\left(w_{so-\text{we}}^{j,k} - w_{so-\text{wa}}^{j,k}\right)w_{so-\text{wa}}^{j,k} + \frac{1}{2}w_{so-\text{wa}}^{j,k}{}^2\right)\right] \tag{7}$$

The external work W_{ext}^k associated to the warp yarn of index k is defined by

$$W_{\text{ext}}^k = W_{\text{traction}}^k + W_{\text{gr}}^k + W_{\text{reaction forces}}^k \tag{8}$$

where

- W_{traction}^k is the work of the traction load P_{wa},
- W_{gr}^k is the work of the gravity load,
- $W_{\text{reaction forces}}^k$ is the work of the reaction forces at the contact points.

The strain energy U_{wa}^k related to the same warp yarn, which takes into account the flexional and the extensional deformation, is expressed in terms of the rotational and extensional parameters (respectively the variables $\psi_{x,i}^k$ and u_i^k, see Fig. 1 in Part I), thus

$$U^k = U_F^k + U_{ex}^k = \sum_{i=1}^{N_d-1} \frac{1}{2} C_{bi}^k \left(\psi_{x,i+1}^k - \psi_{x,i}^k\right)^2 + \sum_{i=1}^{N_d} \frac{1}{2} C_{ei}^k \left(u_{i+1}^k - u_i^k\right)^2 \tag{9}$$

The potential energy V_{wa}^k related to the warp yarn, is then deduced from an analysis similar to that presented in the first part of the paper, using here the double indexing notation, as

$$V_{\text{wa}}^k = \left(\sum_{i=1}^{N_d-1} \frac{1}{2} C_{bi}^k \left(\psi_{x,i+1}^k - \psi_{x,i}^k\right)^2 + \sum_{i=1}^{N_d} \frac{1}{2} C_{ei}^k \left(u_{i+1}^k - u_i^k\right)^2 + \sum_{i=1}^{N_d-1} m_i g \left(w_i^k - w_{oi}^k\right)\right.$$

$$-P_{\text{wa}} \left(\sum_{i=1}^{N_d} \frac{\Delta}{2} \left(\psi_{x,i}^k{}^2 - \psi_{x,oi}^k{}^2\right) + u_{n+1}^k\right) + \sum_{j=1}^{N_{\text{we}}} \frac{\pi^4}{2} \frac{(EI)_{\text{we}}}{\left(L_p^{\text{we}}\right)^3} \left(1 + \frac{\alpha_{\text{we}}}{N_{\text{wa}}^2}\right)$$

$$\left.\times \left[\left(\left(w_{so-\text{we}}^{j,k} - w_{so-\text{wa}}^{j,k}\right)w_{s-\text{wa}}^{j,k} + \frac{1}{2}w_{s-\text{wa}}^{j,k}{}^2\right) - \left(\left(w_{so-\text{we}}^{j,k} - w_{so-\text{wa}}^{j,k}\right)w_{so-\text{wa}}^{j,k} + \frac{1}{2}w_{so-\text{wa}}^{j,k}{}^2\right)\right]\right) \tag{10}$$

The total potential energy associated to the sub-mechanical system Ω_{wa} is finally calculated as the sum of the potential energies of each warp yarn: using Eq. (10), we get

$$V = \sum_{k=1}^{N_{wa}} V^k \tag{11}$$

or in developed form,

$$
\begin{aligned}
V = \sum_{k=1}^{N_{wa}} \Bigg(& \sum_{i=1}^{N_d-1} \frac{1}{2} C_{bi}^k \left(\psi_{x,i+1}^k - \psi_{x,i}^k \right)^2 + \sum_{i=1}^{N_d} \frac{1}{2} C_{ei}^k \left(u_{i+1}^k - u_i^k \right)^2 + \sum_{i=1}^{N_d-1} m_i g \left(w_i^k - w_{oi}^k \right) \\
& - P_{wa} \left(\sum_{i=1}^{N_d} \frac{\Delta}{2} \left(\psi_{x,i}^{k\,2} - \psi_{x,oi}^{k\,2} \right) + u_{n+1}^k \right) + \sum_{j=1}^{N_{we}} \frac{\pi^4}{2} \frac{(EI)_{we}}{\left(L_p^{we} \right)^3} \left(1 + \frac{\alpha_{we}}{N_{wa}^2} \right) \\
& \times \left[\left((w_{so-we}^{j,k} - w_{so-wa}^{j,k}) w_{s-wa}^{j,k} + \frac{1}{2} w_{s-wa}^{j,k\,2} \right) - \left((w_{so-we}^{j,k} - w_{so-wa}^{j,k}) w_{so-wa}^{j,k} + \frac{1}{2} w_{so-wa}^{j,k\,2} \right) \right] \Bigg)
\end{aligned}
\tag{12}
$$

This expression will be used in the sequel to analyze the mechanical behavior of the woven structure, under uniaxial and biaxial behavior.

2. Tensile behavior of the woven structure: traction curve

2.1. Energy description

Each node (with global index i) of warp yarn having the index k is attached the discrete kinematic variables

$$
\begin{cases}
w_{s-wa}^{j,k} = w_i^k \\
\sin \left(\psi_{x,i}^k \right) = \frac{w_i^k - w_{i-1}^k}{\Delta}
\end{cases}
\quad \text{with } i = \frac{(2j-1)N_d}{2N_{we}}
\tag{13}
$$

For small rotations, the relation (13) linking the discrete parameters $\psi_{x,i}^k$ and w_i^k can be approximated by the following expression:

$$\psi_{x,i}^k \approx \frac{w_i^k - w_{i-1}^k}{\Delta} \tag{14}$$

where the discrete lateral displacements w_i^k are obtained from the discretization of the continuous shape of the k-warp yarn, given by the equation

$$\forall i \in [1, N_d - 1], \quad \forall k \in [1, N_{wa}], \quad w_i^k = w_{wa}^k(x_i) = \sum_{p=1}^{N_{we}} a_{p,k}^{wa} \sin \left((k-1)\pi + \frac{p\pi}{L_{wa}} x_i \right) \quad \text{with } x_i = \frac{iL_{wa}}{N_d} \tag{15}$$

Substituting Eqs. (14), (15) into expression (12), the total potential energy V become a function of the Fourier coefficients $\left(a_{p,k}^{wa} \right)_{(p,k) \in [1,...,N_{we}; 1,...,N_{wa}]}$ and of the yarn nodal extensions $\left(u_2^k, u_3^k, \ldots, u_{N_d+1}^k \right)_{k \in [1,...,N_{ch}]}$, viz

$$V = V \left(a_{1,k}^{wa}, \ldots, a_{i,k}^{wa}, \ldots, a_{N_{tr},k}^{wa}, u_2^k, \ldots, u_i^k, \ldots, u_{N_d+1}^k \right)_{k \in [1,...,N_{wa}]} \tag{16}$$

We assume that the woven structure is fixed at the side $x = 0$, which implies the condition

$$\left(u_1^k = 0 \right)_{k \in [1,...,N_{wa}]} \tag{17}$$

The equilibrium state of the sub-mechanical system Ω_{wa} is characterized by the minimum of the total potential energy V; thereby, the first variations of the total potential energy vanish, leading to the following system of algebraic equations:

$$\left(\frac{\partial V}{\partial a_{i,k}^{\text{wa}}}\right)_{(i,k)\in[1,\ldots,N_{\text{we}};1,\ldots,N_{\text{wa}}]} = 0 \quad \text{and} \quad \left(\frac{\partial V}{\partial u_i^k}\right)_{(i,k)\in[2,\ldots,N_{d+1},1,\ldots,N_{\text{wa}}]} = 0 \tag{18}$$

2.2. Fabric under uniaxial extension

2.2.1. Fabric tensile curves

A uniaxial traction is supposed to be exerted in the sole warp direction: this means that in the total potential energy (expression (12)), we set the coefficient $\alpha_{\text{we}} = 0$. The traction curve is generated as the relationship between the load P_{wa} vs. the end nodal displacement (displacement of the free edge $x = L_{\text{wa}}$) along the x-direction. We notice that the traction load P_{wa} is defined as a punctual force applied at the end points of each warp yarn (see Fig. 5 of Part I). The input data correspond to carbon fibers reinforced fabric (SNECMA, 2002), already used in the first part of the paper.

As for the single yarn traction, the obtained simulated J-shape of the fabric tensile response (Fig. 2) is in good agreement with observed experimental results (Boisse et al., 1997). We can distinguish two nearly linear parts, associated to different deformation mechanisms: the first part (up to an applied force of about 0.01 N) is due to the yarn–yarn undulation transfer, traducing a decrease of the warp undulation. At the end of the transfer of undulation (the structure is nearly blocked regarding the variations of undulation), a stiffer response represented by the non-linear part is obtained, due mostly to the extension of the yarn.

2.2.2. Effect of yarns mechanical properties

The reaction load at the interlacing points depends on the weft mechanical parameter, as evidenced by Eq. (4). In order to assess the effect of the mechanical and geometrical characteristics on the fabric traction behavior, simulations of the traction behavior of the fabric in the warp direction are performed for different values of the transverse yarns rigidity. Fig. 3 shows that a stiffer transverse yarn increases the reaction forces, thus leads to a stiffer response of the warp (Fig. 4).

At the end of this stiffening, the reaction force tends toward a limit value, which indicates that the yarn has exhausted its possibilities of undulation changes.

2.3. Fabric under biaxial extension: analysis of the biaxial behavior

We analyze the effect of the transverse extension load P_{we} on the fabric mechanical behavior, in the warp direction (x-direction). We can deduce from Eq. (4) that the reaction force occurring at the interlacing points varies with P_{we}, thus leads to different fabric traction responses.
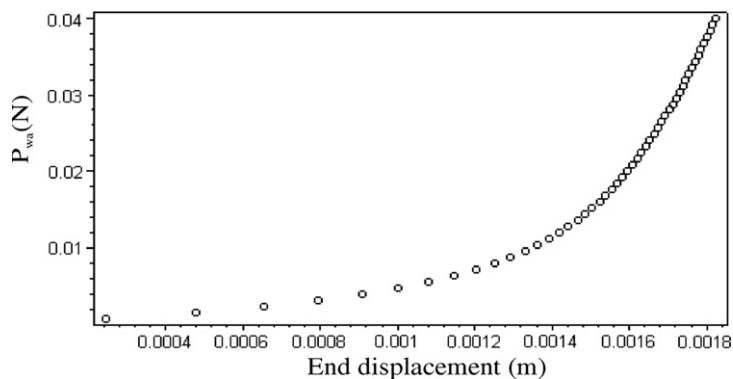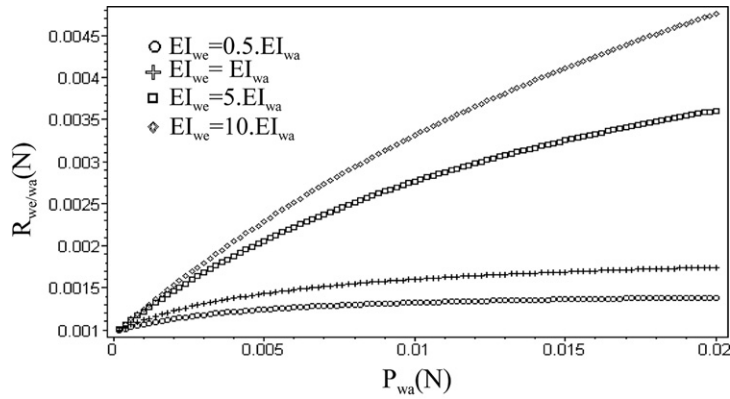

Fig. 2. Uniaxial traction curve.

Fig. 3. Variation of the reaction force. Effect of warp and weft modulus.
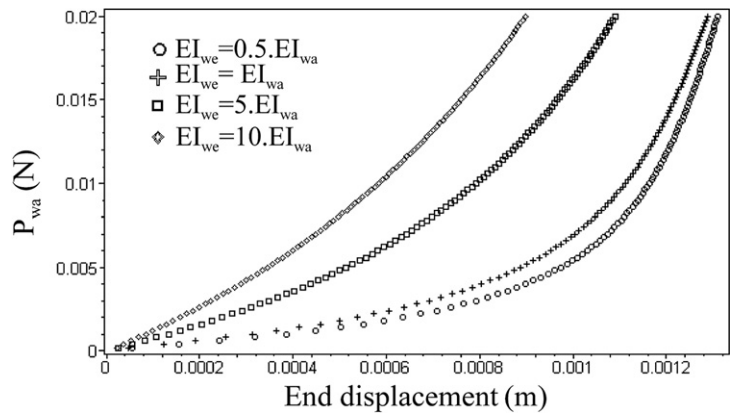

Fig. 4. Fabric extension in the warp direction. Effect of the weft modulus.

2.3.1. Fabric extension response

The followings values of the extension load P_{we} are considered (viewed here as a parameter):

$$\begin{cases} P_{we} = 0.0 P_{wa} \\ P_{we} = 0.1 P_{wa} \\ P_{we} = 0.2 P_{wa} \\ P_{we} = 0.3 P_{wa} \end{cases} \qquad (19)$$

The results (Fig. 5) show that increasing the transverse extension load P_{we} leads to a stiffer response of the fabric: this is due to the decrease of the yarn–yarn undulation transfer capacity. Indeed, from Eq. (4), we remark that as P_{we} increases, the reaction load $R_{we/wa}$ increases, which affects the yarn–yarn undulation transfer, thus leading to a stiffer response. We further record the variation of the reaction load $R_{we/wa}$, occurring at the crossing points, vs. the applied extension load P_{wa} (in the x-direction), considering different values of P_{we} (given in (19)), see Fig. 6.

The reaction force $R_{we/wa}$ increases with the transverse extension load P_{we}. Although the reaction load $R_{we/wa}$ tends toward a limit value in the case of an uniaxial extension ($P_{we} = 0$), we remark that, in the case of biaxial extension, it grows continuously without reaching a limit value: Eq. (4) shows that the reaction force $R_{we/wa}$ not only varies according to the position of the warp/weft yarns' summits, but also according to the transverse extension load P_{we}. In fact, when the yarn–yarn undulation transfer process is exhausted, the reac-
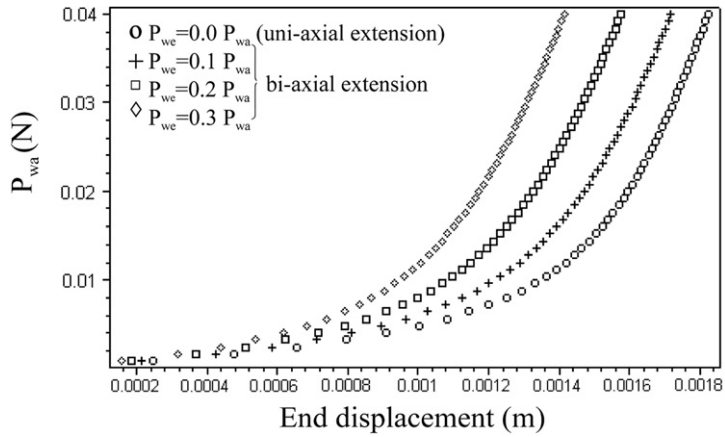
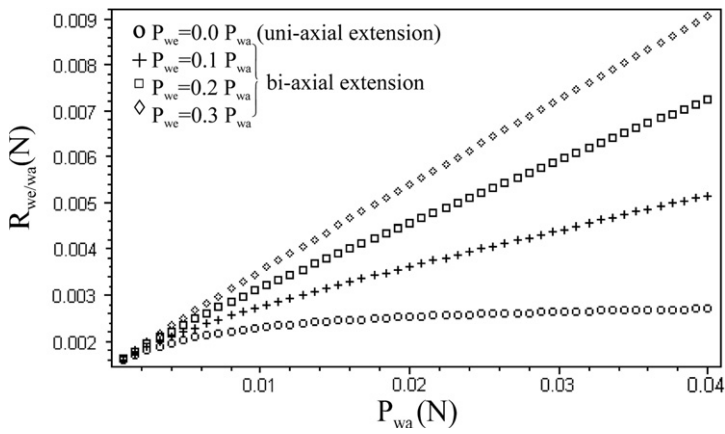Fig. 5. Traction curves: effect of the transverse extension load P_{we}.

Fig. 6. Variation of the reaction load $R_{we/wa}$: effect of the transverse load P_{we}.
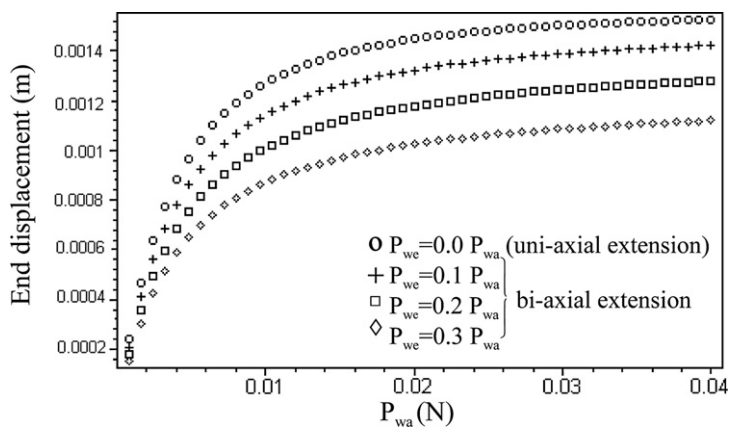

Fig. 7. Variation of the flexional displacement: effect of the transverse load P_{we}.

tion force does not vary any more (since the positions of the contact points between yarns do not change any more); it solely varies vs. P_{we}, with a linear variation that explains the linear part observed on the biaxial traction curves.

2.3.2. Flexional displacement behavior

Fig. 7 illustrates the variation of the flexional displacement (given by Eq. (29a), Part I) vs. the extension load P_{wa}, for the values of the transverse applied traction P_{we} considered in (19): the flexional displacement contribution of the structure decreases as the transverse load P_{we} increases. We notice also that the flexional displacement contribution rapidly reaches a limit value when the transverse load P_{we} is large: indeed, when P_{we} increases, so does also the reaction load (Fig. 7), which leads to rapidly reduce the yarn–yarn undulation transfer.

3. Conclusion

We have developed a discrete mass-spring model of the meso/macro mechanical behavior of a woven structure. This approach takes into account the yarn–yarn interactions at the mesoscopic scale, the effect of which on the macroscopic behavior has been quantitatively assessed. We have shown that the macroscopic behavior of the fabric strongly depends on the mechanical and geometrical yarns parameters and also on the ratio of the biaxial loading. The contribution to the total deformation of the flexional displacement (due to the undulations variation) and of the extensional displacement (due to the yarns stretching) during the fabric extension has been analyzed. The flexional displacement is shown to tend towards a saturation value, whereas the extensional displacement monotonously increases vs. the applied traction load.

The consideration of the yarns compressibility and the extension of the discrete approach to more complex armors (such as serge, satin, or even three-dimensional weaving) constitutes the main perspective of development of the discrete modeling strategies of fabric.

References

Boisse, P., Borr, M., Buet, K., Cherouat, A., 1997. Composites Part B 28B, 453–464.
Magno, M., Lutz, R., 2002. European Journal of Mechanics A/Solids 21, 669–682.
Provot, X., 1995. Deformation constraints in a mass-spring model to describe rigid cloth behavior. Graphics Interface, 147–155.
SNECMA Moteurs. Le Haillan, France. Internal Report, 2002.
Timoshenko, S., 1947. Théorie de la Stabilité Elastique. BERANGER, Paris & Liège.